Amplitude analyses for exotic meson spectroscopy

Vanamali Shastry

CEEM, Indiana University Bloomington

On behalf of JPAC

Photoproduction Studies on the Deuteron in Hall-D,
April 20, 2026

Hadron spectroscopy

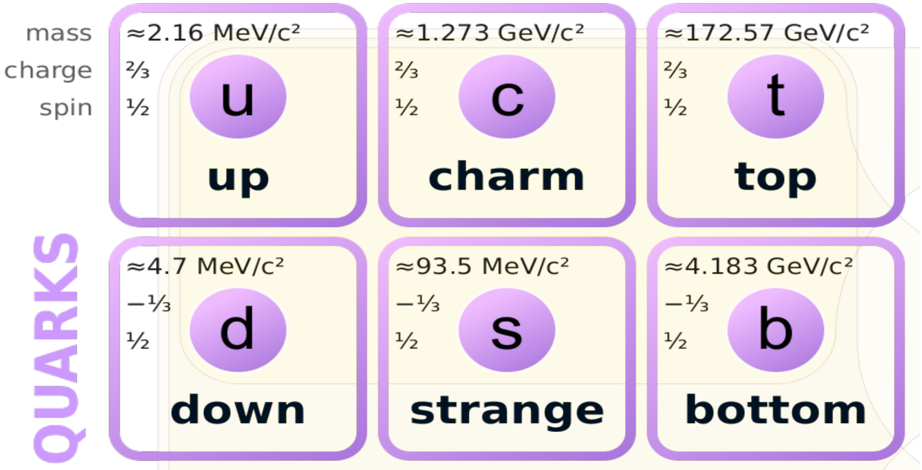

Cush, Public domain, via Wikimedia Commons

- A plethora of states formed by quarks and gluons
- Mesons ($\bar{q}q$) and baryons (qqq) are conventional hadrons
- Other unconventional states possible and observed
  - Hybrids ($\bar{q}qg$) e.g: $\pi_1(1600), \eta_1(1855)$
  - Tetraquarks ($\bar{q}q\bar{q}q$), pentaquarks ($\bar{q}q\bar{q}qq$), hexaquark states ($qqqqqq$), etc e.g: T_{cc}^{+}, and other T_{xx} states, P_{xx} states, etc.
  - Glueballs gg, ggg, etc
  - Molecular states
- Many have been observed, many more yet to be found
- COMPASS, BESIII, LHCb, GlueX, and more!

- Standard model provides six quarks and a force carrier (gluon)
- Fundamental states of QCD can have three possible charges (colors)
  - Only color neutral states are observable (hadrons)
  - Confinement and asymptotic freedom

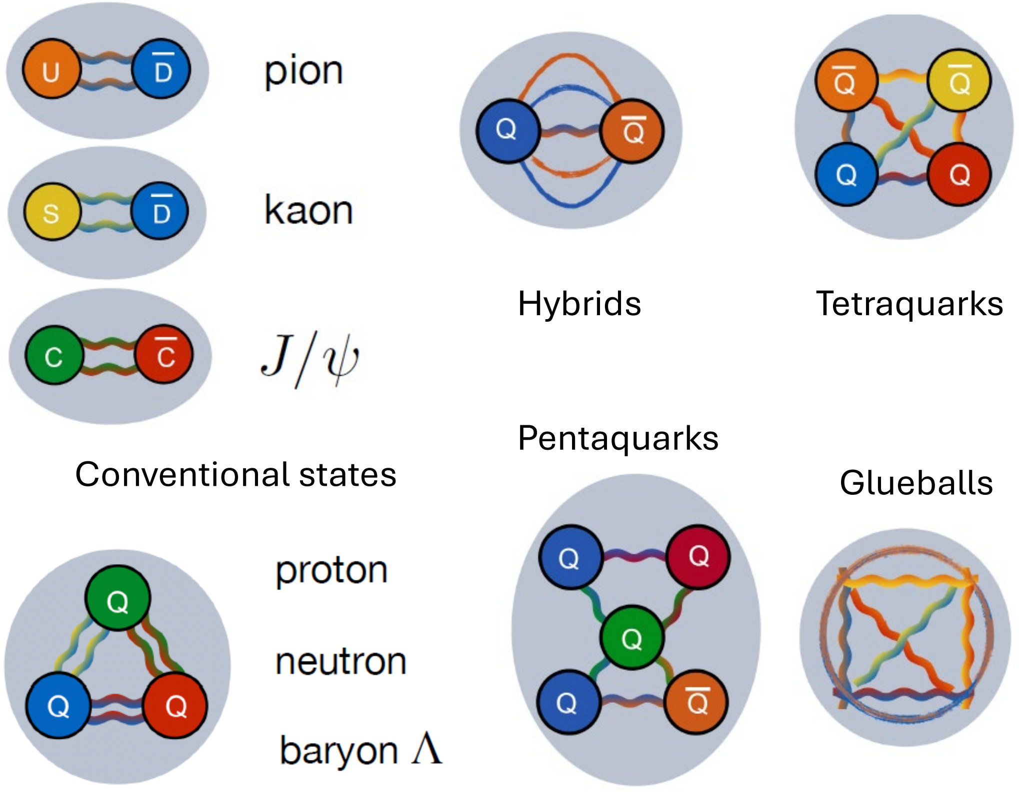

Courtesy: Vincent Mathieu, U. Barcelona

Hadron spectroscopy

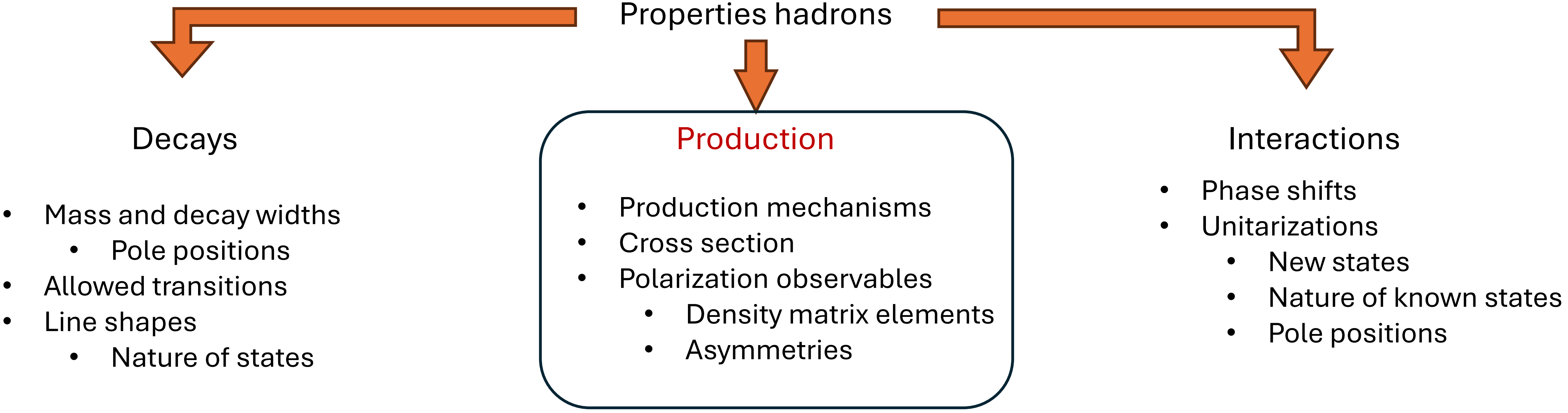

Properties hadrons

Decays

- Mass and decay widths
  - Pole positions
- Allowed transitions
- Line shapes
  - Nature of states

Production

- Production mechanisms
- Cross section
- Polarization observables
  - Density matrix elements
  - Asymmetries

Interactions

- Phase shifts
- Unitarizations
  - New states
  - Nature of known states
  - Pole positions

Joint Physics Analysis Center (JPAC)

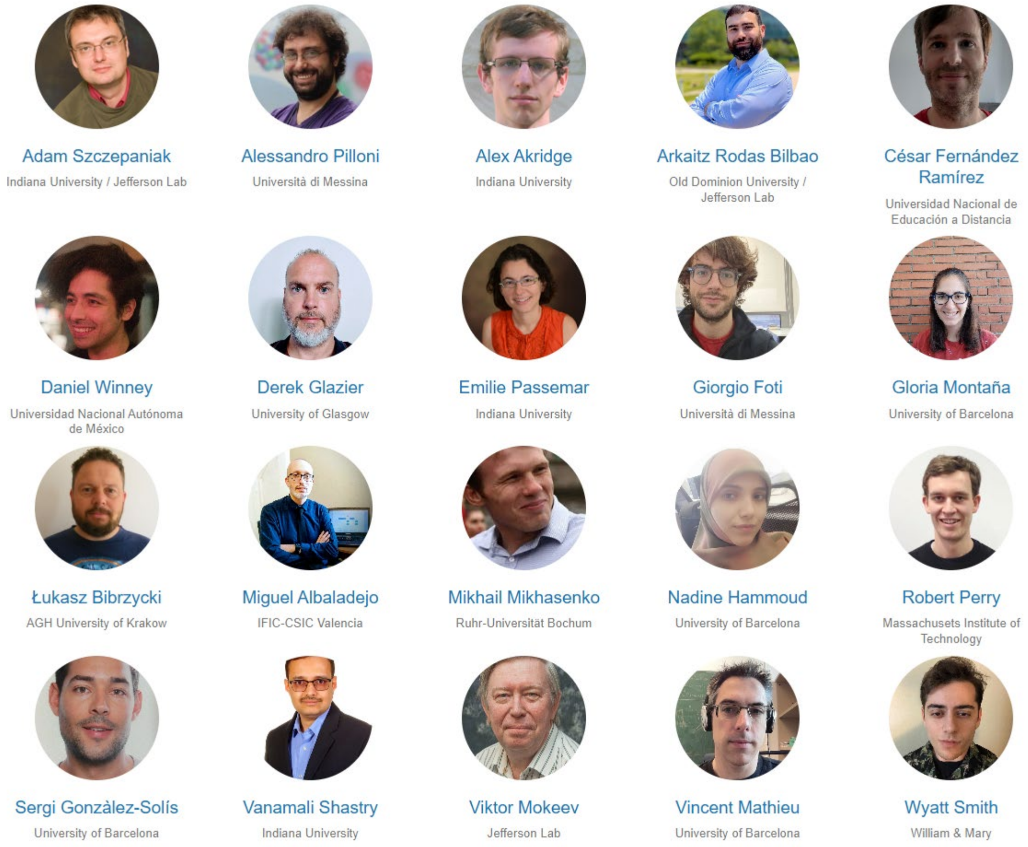

Adam Szczepaniak
Indiana University / Jefferson Lab

Alessandro Pilloni
Università di Messina

Alex Akridge
Indiana University

Arkaitz Rodas Bilbao
Old Dominion University / Jefferson Lab

César Fernández Ramírez
Universidad Nacional de Educación a Distancia

Daniel Winney
Universidad Nacional Autónoma de México

Derek Glazier
University of Glasgow

Emilie Passemar
Indiana University

Giorgio Foti
Università di Messina

Gloria Montaña
University of Barcelona

Łukasz Bibrzycki
AGH University of Krakow

Miguel Albaladejo
IFIC-CSIC Valencia

Mikhail Mikhasenko
Ruhr-Universität Bochum

Nadine Hammoud
University of Barcelona

Robert Perry
Massachusetts Institute of Technology

Sergi Gonzàlez-Solís
University of Barcelona

Vanamali Shastry
Indiana University

Viktor Mokeev
Jefferson Lab

Vincent Mathieu
University of Barcelona

Wyatt Smith
William & Mary

Full members

Phenomenology Lattice AI/ML

- Emphasize the need for amplitude analysis
- Pole positions extracted from data included in PDG
  - $a_2(1320), a_2(1700), \pi_1(1600)$ (Rodas, *et al* PRL 122 (2019) 4, 042002)
- Production mechanisms
  - $\pi\pi$ production at large energies
  - $\eta\pi$ production at large energies and double Regge exchange
  - More complicated photoproduction processes

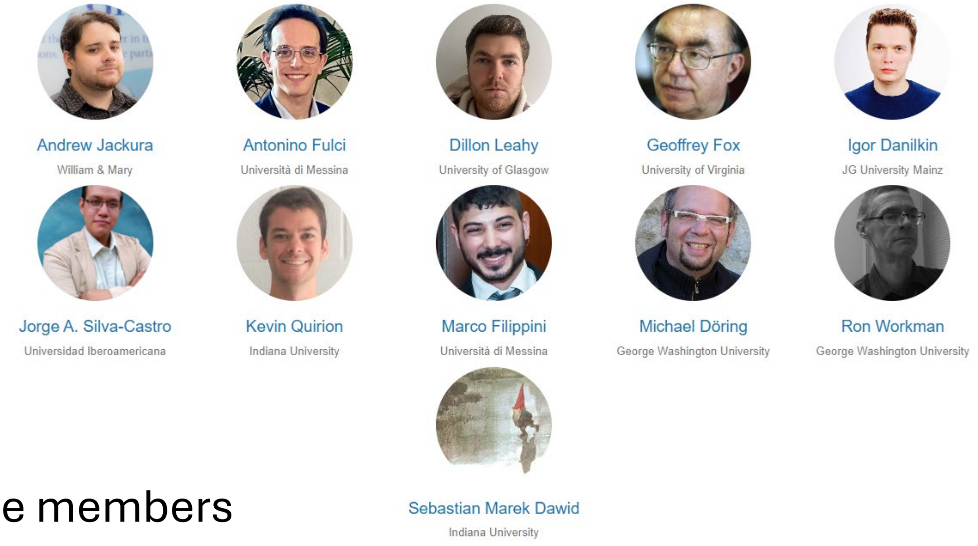

Andrew Jackura
William & Mary

Antonino Fulci
Università di Messina

Dillon Leahy
University of Glasgow

Geoffrey Fox
University of Virginia

Igor Danilkin
JG University Mainz

Jorge A. Silva-Castro
Universidad Iberoamericana

Kevin Quirion
Indiana University

Marco Filippini
Università di Messina

Michael Döring
George Washington University

Ron Workman
George Washington University

Sebastian Marek Dawid
Indiana University

Affiliate members

Amplitude analysis

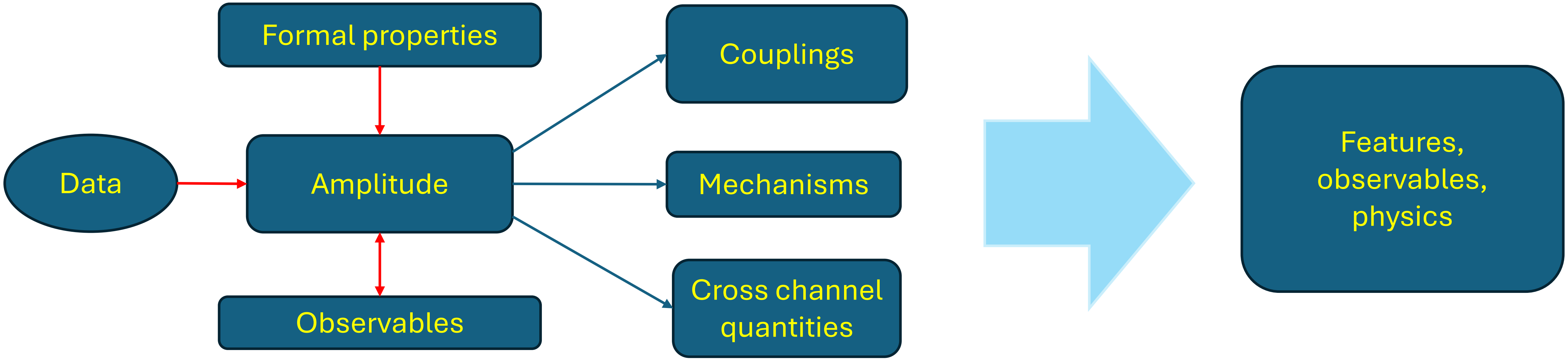

Formal properties

Data

Amplitude

Observables

Couplings

Mechanisms

Cross channel quantities

Features, observables, physics

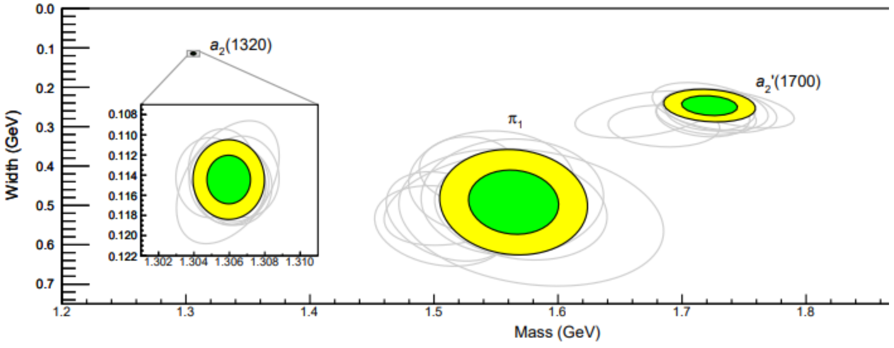

Pole positions of $\eta\pi$ resonances (Phys.Rev.Lett. 122 (2019) 042002)

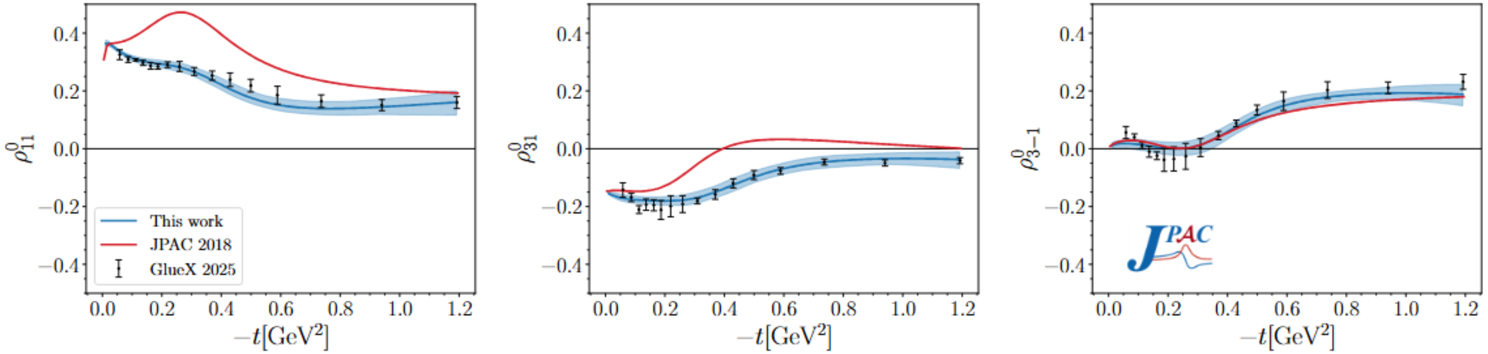

Photoproduction of $\pi\Delta$, *(expected on arXiv this week)*

Production mechanisms

Goal: understand the mechanism behind the photoproduction of $\pi_1(1600)$

- Large-s production of resonances
  - GlueX: $\vec{\gamma} + p \ \rightarrow X^- + \Delta^{++}$; $s \approx 17\ GeV^2$
  - Broad features known from analysis of cross sections; finer details to be understood
  - Pion exchange dominates
  - Relative phases of amplitudes fixed from SDME data

Charge exchange mechanism dominates the production process

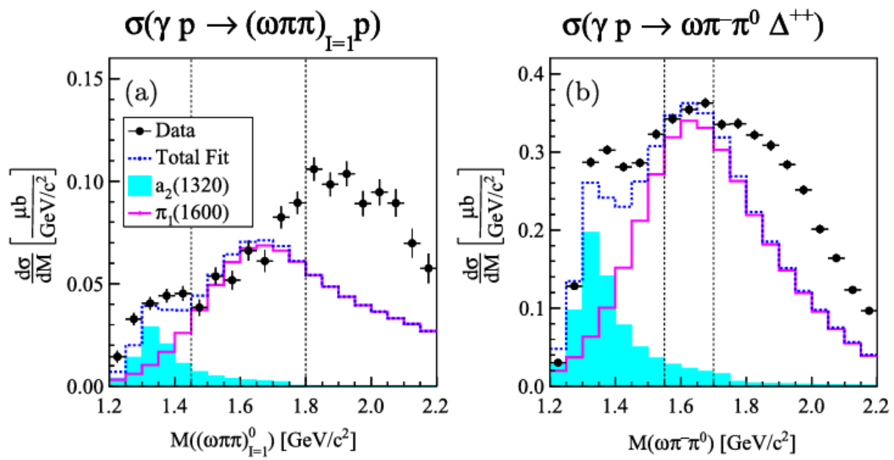

GlueX, *Phys.Rev.Lett.* 133 (2024) 26, 261903

Why is the $\pi_1(1600)$ more likely to be produced in a charge exchange reaction?

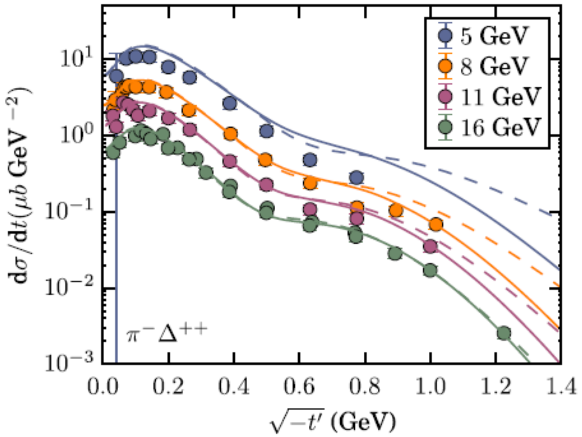

J. Nys *et al* (JPAC): *Phys.Lett.B* 779 (2018) 77-81

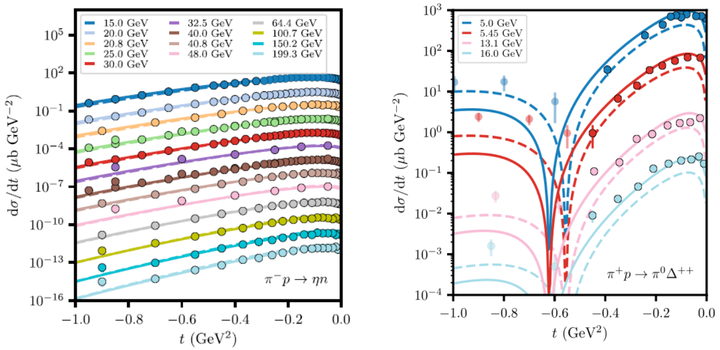

J. Nys *et al* (JPAC), *Phys.Rev.D* 98 (2018) 3, 034020

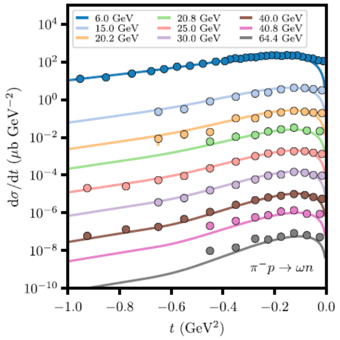

Production mechanisms

Goal: understand the mechanism behind the photoproduction of $\pi_1(1600)$

How does this compare with neutron targets?

$$\gamma + n \rightarrow \pi_1^- + p$$

versus

$$\gamma + p \rightarrow \pi_1^- + \Delta^{++}$$

Charge exchange mechanism dominates the production process

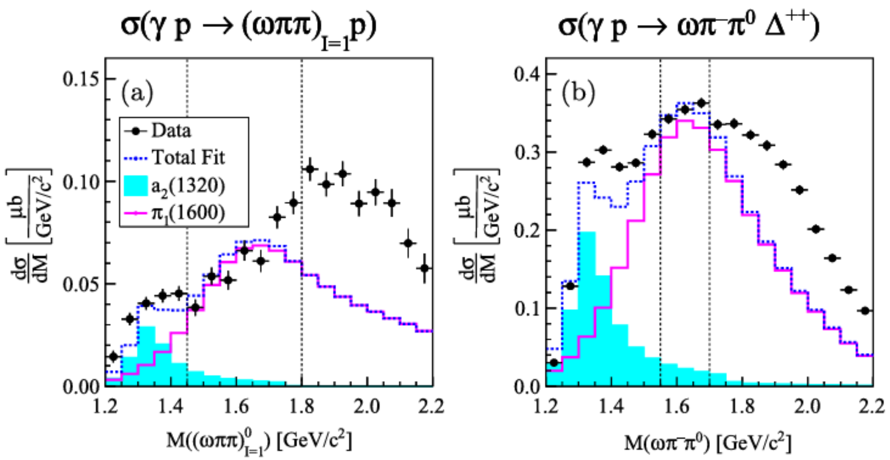

GlueX, *Phys.Rev.Lett.* 133 (2024) 26, 261903

Why is the $\pi_1(1600)$ more likely to be produced in a charge exchange reaction?

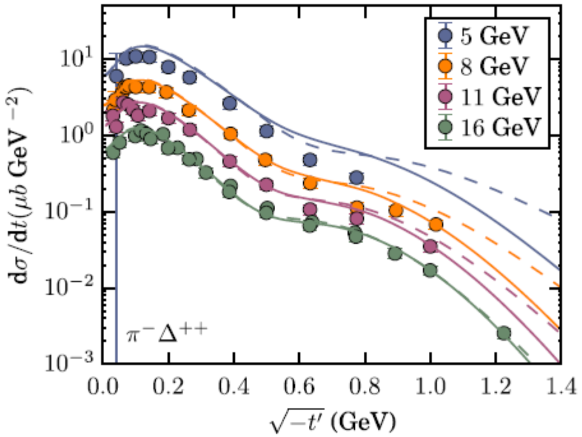

J. Nys *et al* (JPAC): *Phys.Lett.B* 779 (2018) 77-81

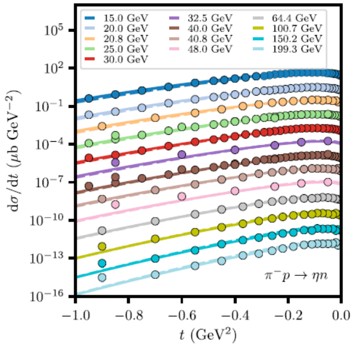

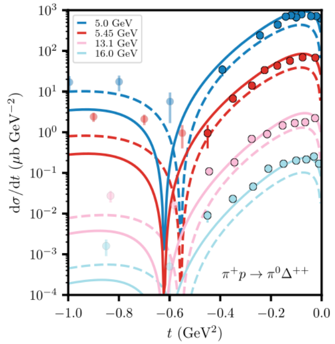

J. Nys *et al* (JPAC), *Phys.Rev.D* 98 (2018) 3, 034020

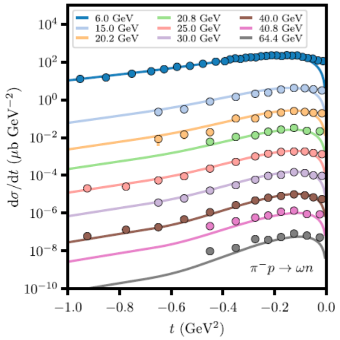

Single pion photoproduction (G. Montaña *et al* (JPAC) *Phys.Rev.D* 110 (2024) 11, 114012)

Reggeization and gauge invariance

- The pion exchange amplitude in the *t*-channel rest frame vanishes.
  - How to explain gauge invariance?
- Pion exchange contributions are “hidden” among other J^P = (even)$^-$ exchanges.
  - Recovered from spin-*J* exchange via analytical continuation
  - Interpreted as cross-channel contributions
- Nucleon and pion poles are connected by gauge invariance
  - *s*- and *u*-channel exchanges are essential to conserve the current at the level of the Born diagrams
  - This carries over to the Regge limit as well.

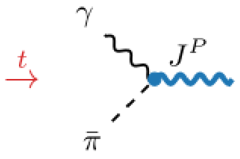

$$A^{\mathrm{e}}_{\mu_\gamma\mu_i\mu_f} = 2\sqrt{2}g_{\pi NN}\left[e_\pi\left(\frac{\epsilon\cdot(p_\pi-k/2)}{t-m_\pi^2}+\frac{\epsilon\cdot P}{s-u}\right)+\frac{1}{2}e_{N_i}\left(\frac{\epsilon\cdot p_\pi}{s-m_N^2}+\frac{\epsilon\cdot P}{s-u}\frac{t-m_\pi^2-k^2}{s-m_N^2}\right)\right.$$
$$\left.-\frac{1}{2}e_{N_f}\left(\frac{\epsilon\cdot p_\pi}{u-m_N^2}+\frac{\epsilon\cdot P}{s-u}\frac{t-m_\pi^2-k^2}{u-m_N^2}\right)\right]\bar{u}(p_f,\mu_f)\gamma_5 u(p_i,\mu_i).$$

Born amplitude

$$\mathcal{A}^{J\to 0}(s,t) = i\,\frac{\alpha'}{\alpha(t)}\frac{z_t}{\sqrt{1-z_t^2}}$$

t-channel pion exchange amplitude obtained via analytical continuation (excluding the Regge propagator)

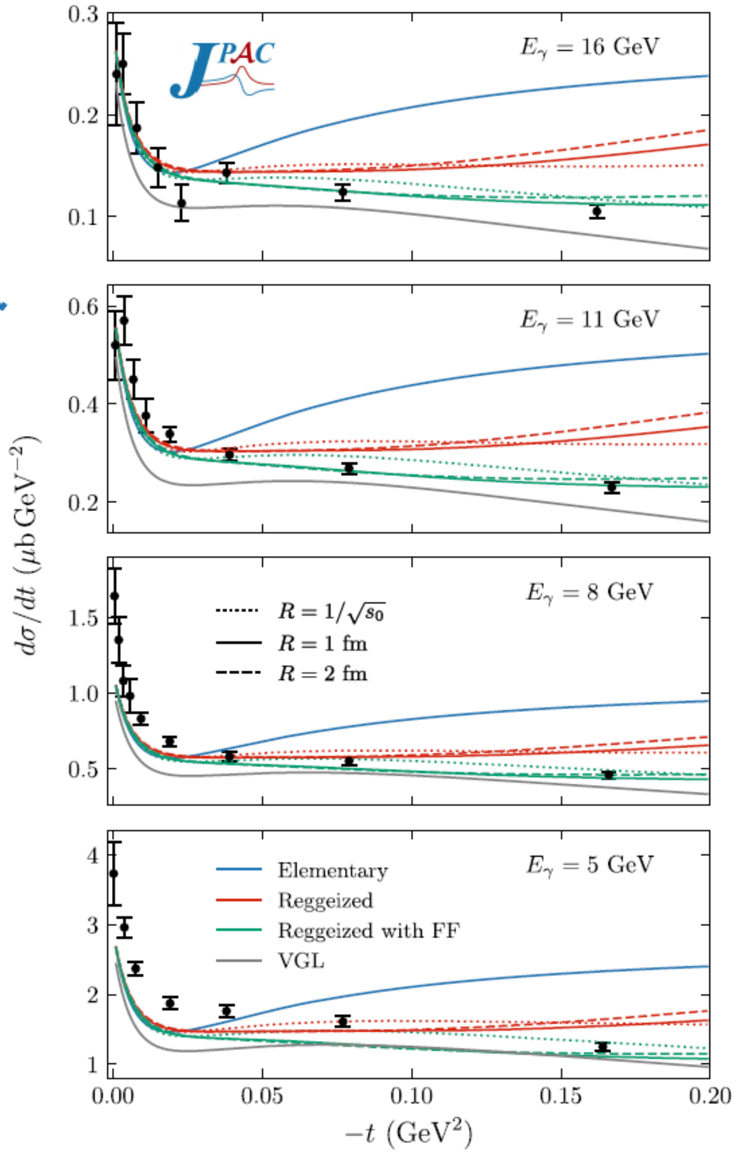

Two pion photoproduction – Vector meson (V. Mathieu *et al* *Phys.Rev.D* 97 (2018) 9, 094003)

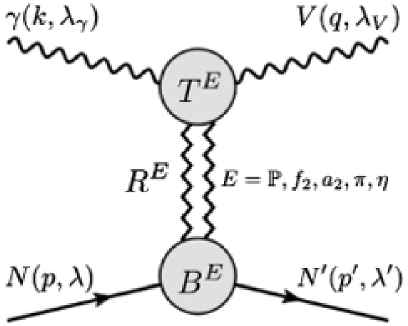

Spin density matrix elements when the $\pi\pi$ is a vector meson

- Dominated by Pomeron exchange.
- Pomeron coupling constants estimated using SLAC data on SDMEs and PDG data on proton and deuteron Compton scattering

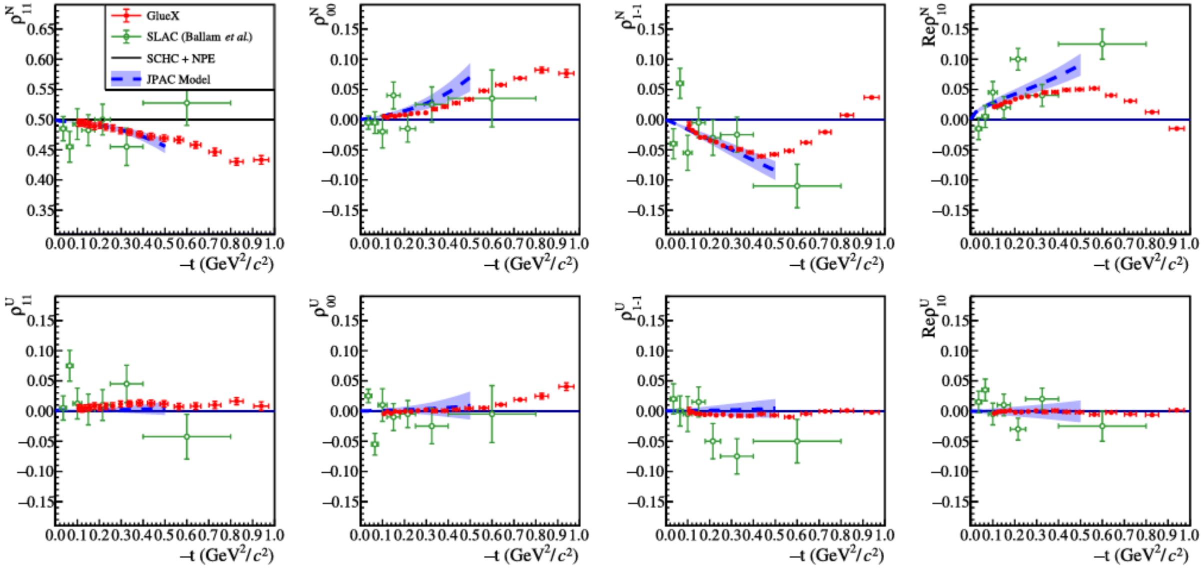

Natural and Unnatural parity exchange SDMEs. JPAC model compared to GlueX and SLAC data. GlueX, *Phys.Rev.C* 108 (2023) 5, 055204

- The model explains the SLAC data quite well
- Pomeron dominance implies dominant natural exchange contributions
- The model was used a prediction for GlueX measurements
- The GlueX data for the SDMEs in the small $|t|$ region is very well explained by the model.

How would these compare to charge exchange process?

Two pion photoproduction – $\pi\Delta$ (V. Shastry *et al* (JPAC) *on the way to arXiv*)

Spin density matrix elements when one of the pions comes from the lower vertex

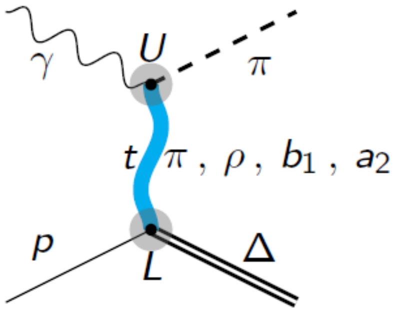

- Amplitude factorizes at large s.
- Base model has vertices modelled using effective Lagrangians.
    - Production cross sections, and beam asymmetries are well explained
    - Unnatural parity exchange dominates the small $|t|$ region and natural parity exchange dominates the large $|t|$ region

$$T_{\lambda_\gamma,\lambda_1,\lambda_\Delta}(s,t) = \sum_{\times}\left[\xi_{\lambda_\gamma\lambda_1\lambda_\Delta}\, T^{\times}_{\lambda_\gamma,\lambda_1,\lambda_\Delta}(s,t)\right] \; ; \qquad \times \in \{\pi, \rho, b_1, a_2\}$$

$$T^{\times}_{\lambda_\gamma,\lambda_1,\lambda_\Delta}(s,t) = \sqrt{-t}^{\;|\lambda_\gamma|}\sqrt{-t}^{\;|\lambda_1-\lambda_\Delta|}\;\hat{\beta}^{\times,U}_{\lambda_\gamma}(t)\;\hat{\beta}^{\times,L}_{\lambda_1,\lambda_\Delta}(t)\;\mathcal{P}^{\times}_{R}(s,t)\;\mathcal{S}_{\times}(t)$$

- Relative phases (including the signs of $\beta_{\lambda_1\lambda_\Delta}$) unconstrained by cross section alone
    - SDMEs solve most of this problem
- Needs a reparameterization of the model

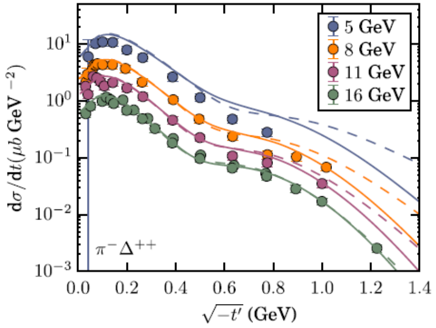

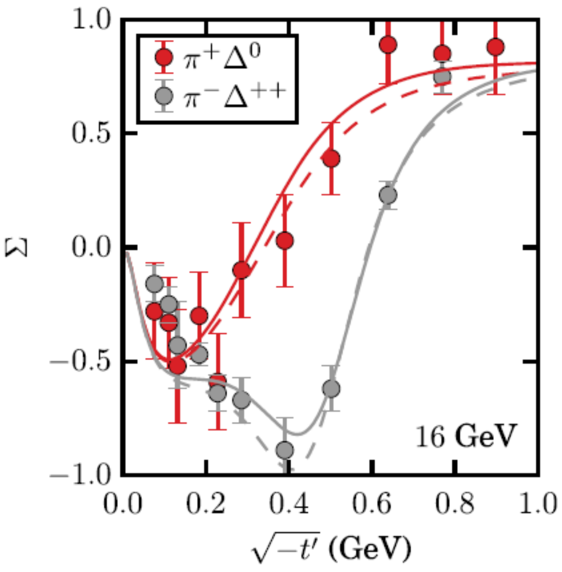

J. Nys *et al* (JPAC):
Phys.Lett.B 779 (2018) 77-81

Two pion photoproduction – $\pi\Delta$ (V. Shastry *et al* (JPAC) *on the way to arXiv*)

Spin density matrix elements when one of the pions comes from the lower vertex

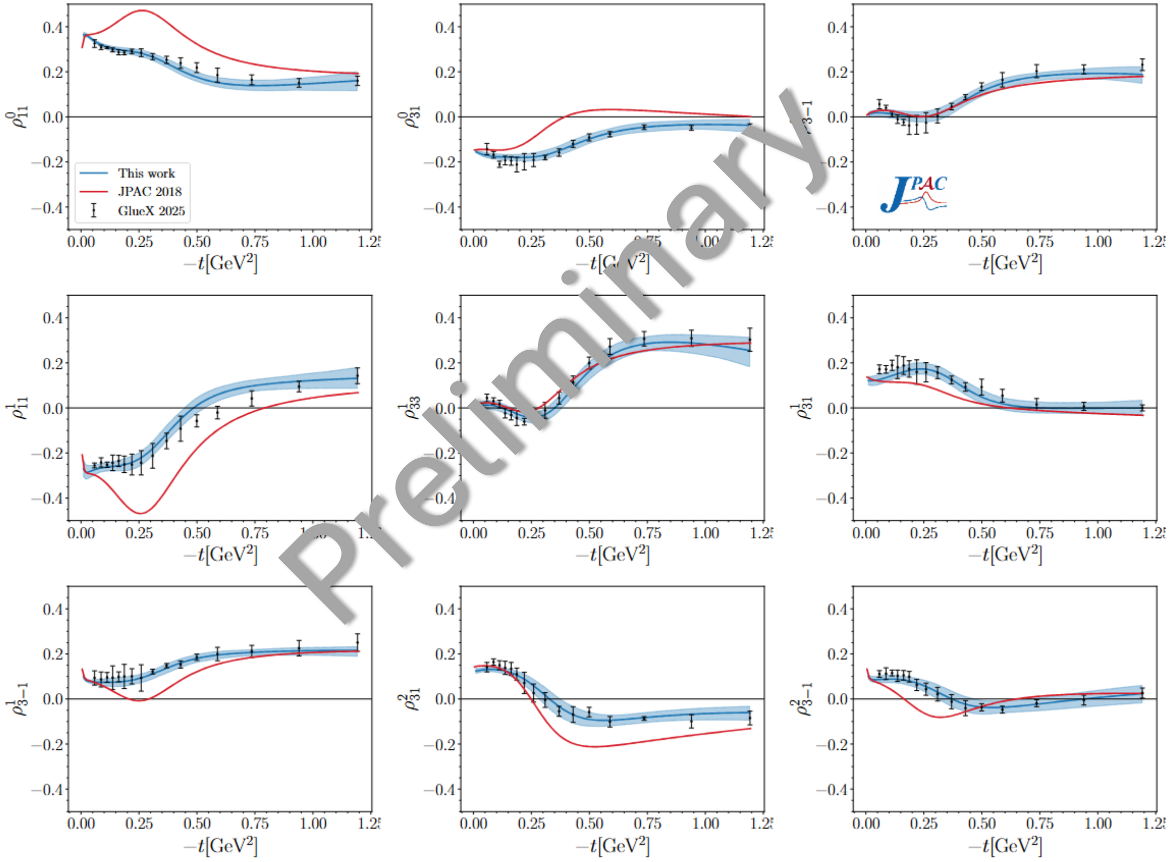

- Instead of Lagrangians, chose polynomials (linear in *t*).
- Fit the coefficients to the data
  - Takes care of any higher order term left out of the model.
- Can be used in any future work involving Δ
- EXD broken for natural exchange
- Very forward region ($|t| \leq\ 0.1\ GeV^2$) shows absorption
- Not effectively described by PMA
- More analysis needed and in progress.

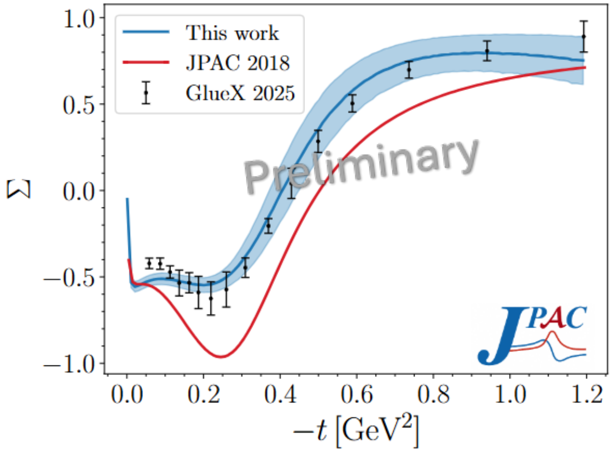

GlueX data from F. Afzal *et al* (GlueX), *Phys.Lett.B* 863 (2025) 139368

Two pion photoproduction – $\pi\Delta$ (V. Shastry *et al* (JPAC) *on the way to arXiv*)

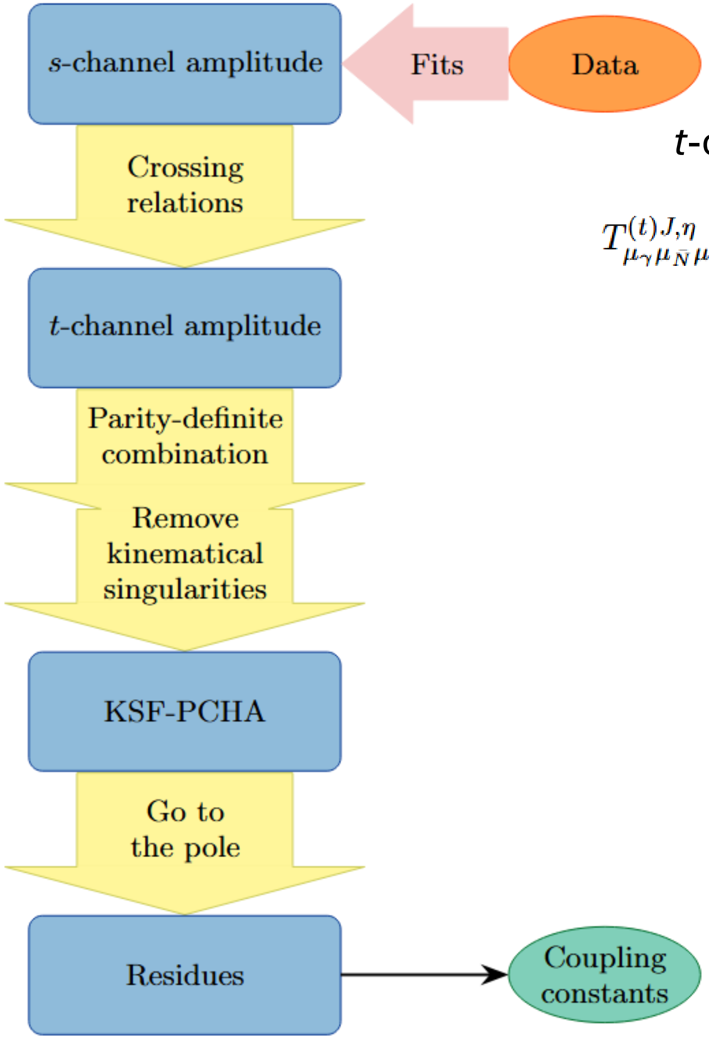

t-channel partial wave amplitude:

$$T^{(t)J,\eta}_{\mu_\gamma\mu_{\bar{N}}\mu_\Delta}(t,s) = \underbrace{\mathcal{K}_{\mu_\gamma\mu_{\bar{N}}\mu_\Delta}(t)\,\xi^{(t)}_{\mu_\gamma\mu_{\bar{N}}\mu_\Delta}(t,s)}_{\text{Kinematical factors}}\,\underbrace{\mathcal{R}^{J\eta}_{\mu_\gamma\mu_{\bar{N}}\mu_\Delta}(t)\frac{s^J}{t-m_J^2}}_{\text{Dynamical information}}$$

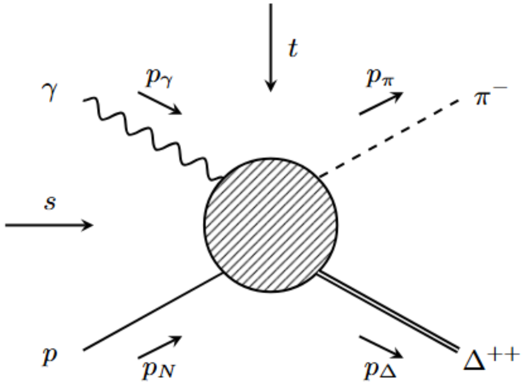

$$\mathscr{R}^{J\eta}_{\mu_\gamma\mu_{\bar{N}}\mu_\Delta} = \lim_{t\to m_J^2}\mathcal{R}^{J\eta}_{\mu_\gamma\mu_{\bar{N}}\mu_\Delta}(t)$$

$$f_{\pi N\Delta} = -2.18 \pm 0.08$$

$$\Gamma_{\pi N\Delta} = 129 \pm 9 \text{ MeV}$$

$\mu_{\bar{N}}$	μ_Δ	$\mathscr{R}^{\pi}_{1\mu_{\bar{N}}\mu_\Delta}$		$\mathscr{R}^{\rho}_{1\mu_{\bar{N}}\mu_\Delta}$		$\mathscr{R}^{b_1}_{1\mu_{\bar{N}}\mu_\Delta}$		$\mathscr{R}^{a_2}_{1\mu_{\bar{N}}\mu_\Delta}$	
		This work	Ref. [21]	This work	Ref. [21]	This work	Ref. [21]	This work	Ref. [21]
$\frac{1}{2}$	$\frac{3}{2}$	—	—	-8.0 ± 2.4	-12.6	4 ± 7	140.1	45 ± 16	31.7
$\frac{1}{2}$	$\frac{1}{2}$	-57.0 ± 2.2	-60.2	-5.3 ± 1.5	-0.05	14.7 ± 14.5	84.5	38 ± 15	3.74
$-\frac{1}{2}$	$\frac{3}{2}$	—	—	—	—	—	—	5.3 ± 4.0	0.0
$-\frac{1}{2}$	$\frac{1}{2}$	—	—	16.0 ± 3.7	-6.62	57 ± 30	144.0	-17 ± 9	11.7

Two pion photoproduction – $\pi\Delta$ (V. Shastry *et al* (JPAC) *on the way to arXiv*)

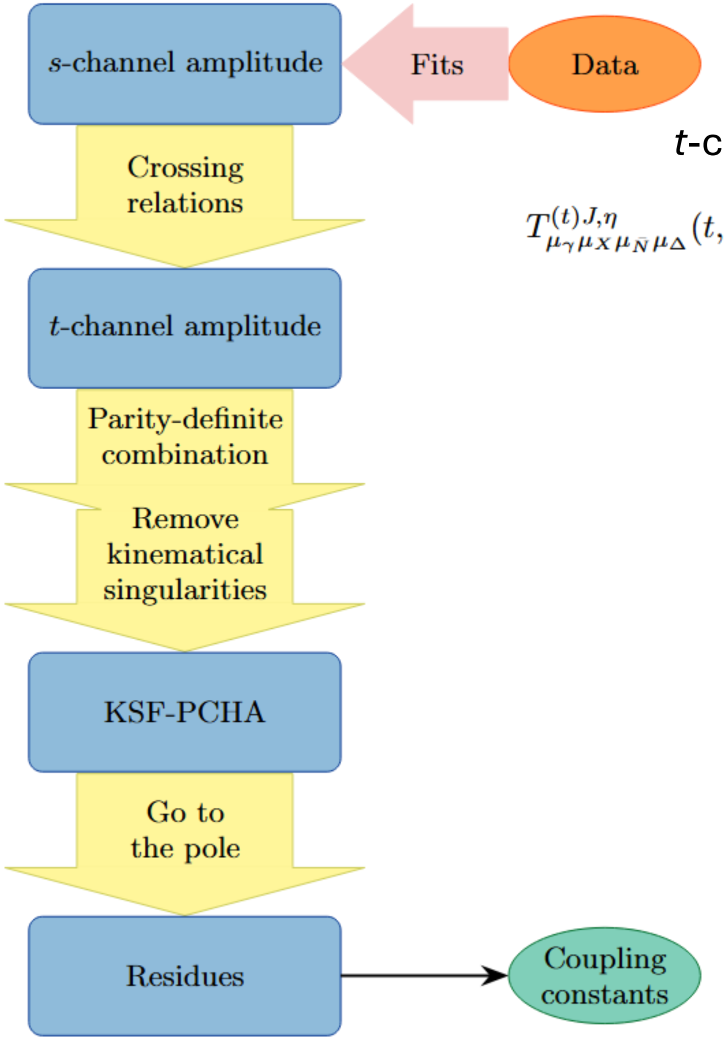
s-channel amplitude

Fits

Data

Crossing relations

t-channel amplitude

Parity-definite combination

Remove kinematical singularities

KSF-PCHA

Go to the pole

Residues

Coupling constants

t-channel partial wave amplitude:

$$T^{(t)J,\eta}_{\mu_\gamma\mu_X\mu_{\bar{N}}\mu_\Delta}(t,s) = \underbrace{\mathcal{K}_{\mu_\gamma\mu_X\mu_{\bar{N}}\mu_\Delta}(t)\,\xi^{(t)}_{\mu_\gamma\mu_X\mu_{\bar{N}}\mu_\Delta}(t,s)}_{\text{Kinematical factors}}\,\underbrace{\mathcal{R}^{J\eta}_{\mu_\gamma\mu_X\mu_{\bar{N}}\mu_\Delta}(t)\frac{s^J}{t-m_J^2}}_{\text{Dynamical information}}$$

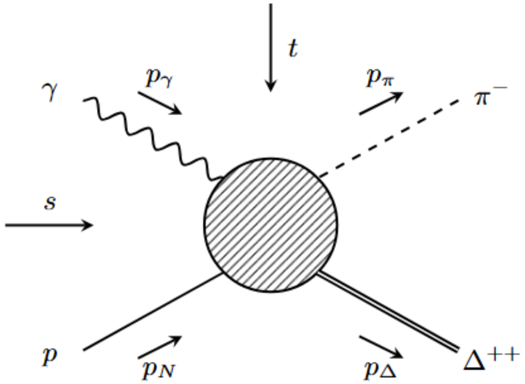

$$\mathscr{R}^{\pi} = \beta^{\pi X\gamma} \times \beta^{\pi\bar{N}\Delta}$$

(For the photoproduction of any meson X)

$$\boxed{\beta^{J\bar{N}N} = \left(\frac{\text{Residue from } \gamma n \to X^- p}{\text{Residue from } \gamma p \to X^-\Delta^{++}}\right) \times \beta^{J\bar{N}\Delta}}$$

Other mesons - a_2, f_2 (V. Mathieu *et al* (JPAC) *Phys.Rev.D* 102 (2020) 014003)

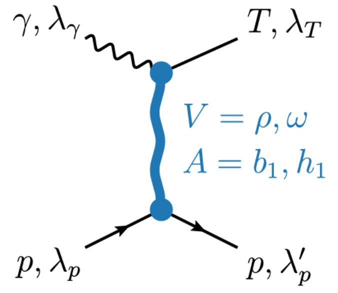

- Vector and axial vector couplings to $T\gamma$ system
- Minimal model has only the momentum independent couplings
  - Gauge invariance to be imposed explicitly
- Tensor meson dominance (TMD) model has vector couplings from the full gauge invariant Lagrangian
- Both models are fit to the CLAS a_2 photoproduction cross section data, f_2 photoproduction cross section is the prediction
- TMD required to explain the dip in the a_2 production cross section
- Unnatural parity exchanges dominate the production mechanism according to the minimal model
  - Counterintuitive to phenomenological predictions, corrected by TMD
- TMD over-estimates f_2 production cross section

Recent results from GlueX support TMD predictions for cross section

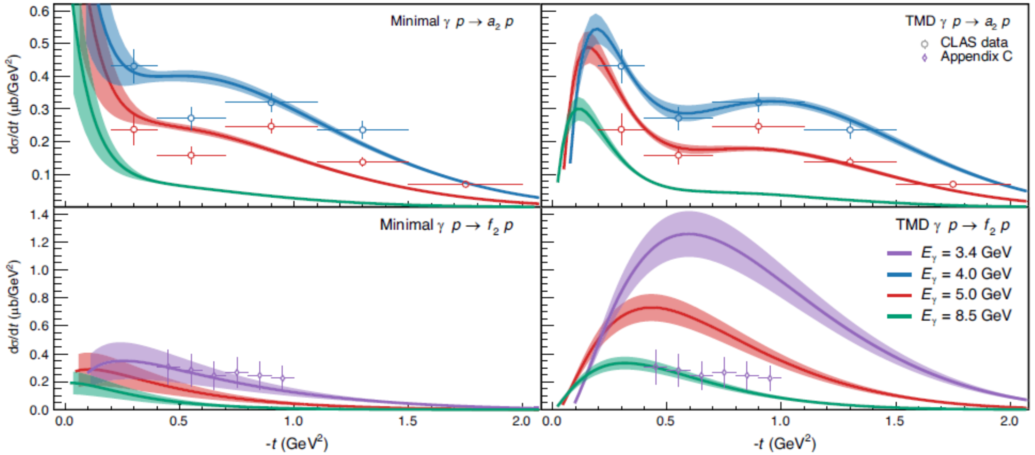

Two models for a_2 and f_2 photoproduction (Phys.Rev.D 102 (2020) 014003), data from CLAS (Phys.Rev.C 102, 032201 (2020))

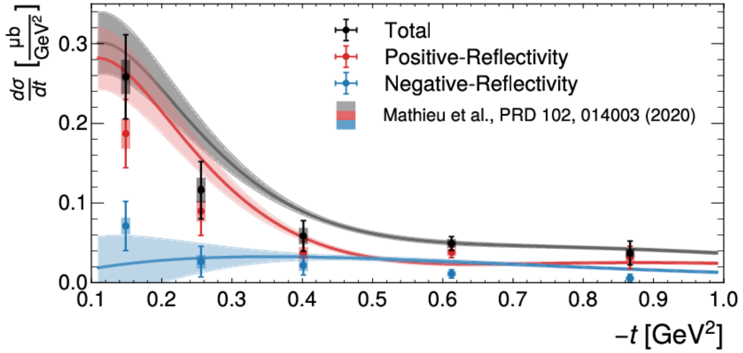

$a_2^0(1320)$ production cross section F. Afzal *et al* (GlueX), *Phys.Rev.C* 112 (2025) 1, 015204

Non-resonant productions – $\eta^{(\prime)}\pi$

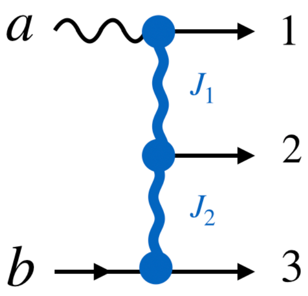

Non-resonant production of two pseudoscalar mesons

Double Regge exchange in $\pi^- + p \to \eta^{(\prime)}\pi^- p$

(EPJC, (2021) 81:647)

- Three models examined:
  - Minimal model with $a_2P + a_2f_2 + f_2f_2$
  - $MIN + f_2P$
  - $MIN + PP$
- Models fitted to COMPASS partial wave data.
- All three models explain the forward region equally well
- Minimal model insufficient to explain the broad backward peak in the $\eta' p$ production
  - $MIN + PP$ gives the broadest backward peak

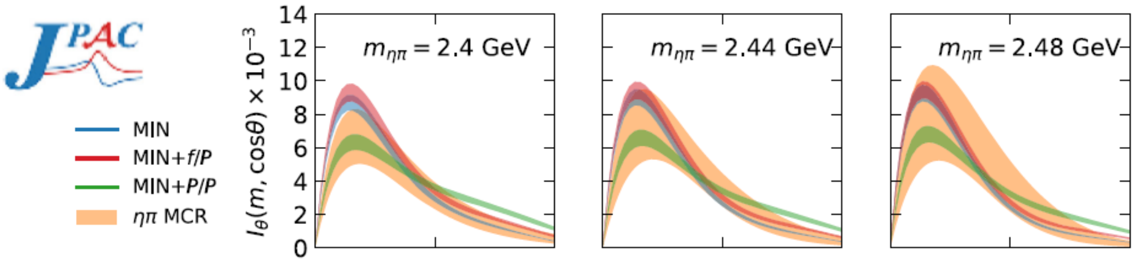

Intensity vs $cos\theta$: Model results (EPJC, (2021) 81:647) compared with COMPASS data (Phys. Lett. B **740**, 303 (2015)).

- Forward – backward asymmetry (FBA) is larger for $\eta'\pi$ than $\eta\pi$

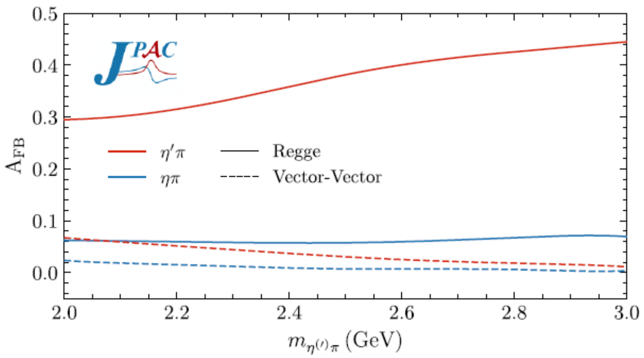

Enhanced coupling of $\eta'\pi$ to $\pi_1(1600)$

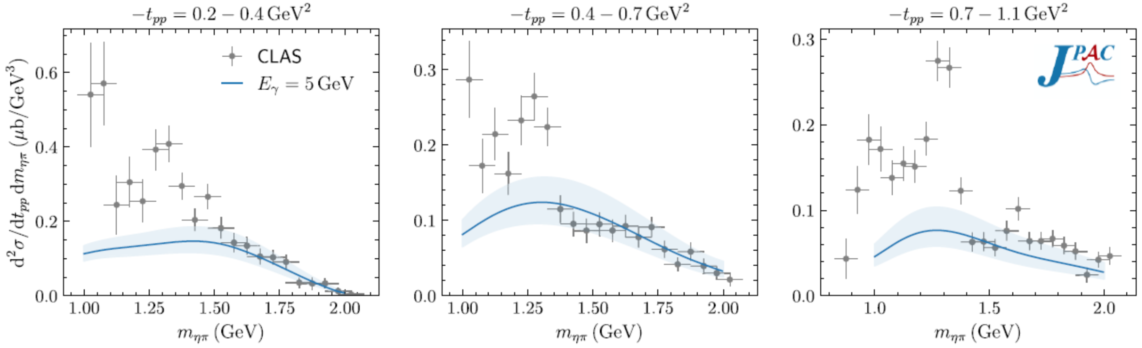

Double Regge exchange in photoproduction of $\eta^{(\prime)}\pi$: Our analysis (G. Montaña, *et al* (JPAC), *Phys.Lett B* 872 (2026) 140101 compared to CLAS data

Summary and future directions

- Understand the underlying mechanism in the high energy photoproduction of mesons
- Provide predictions that can be tested in ongoing and future experiments
  - Data driven modeling
  - Many predictions tested and validated
- Close collaboration with experimentalists on each of these projects
- Residues extracted from $\pi\Delta$ production amplitude
- Interesting physics from $\eta\pi$ system in the form of double Regge exchanges
- All analyses with the goal of modeling $\pi_1\Delta$ and $\pi_1 p$ photoproduction

- Exciting opportunity with a deuteron target
- Charge exchange mechanism may be more readily observable with a neutron target
  - Simpler lower vertex
- Amplitude analysis can lead to interesting physics
  - Production mechanisms – single Regge, double Regge, etc
  - Residues – Couplings of various resonances to $\bar{N}N$ systems.